Scientia Iranica, Vol. 13, No. 4, pp 348 354

SCIENTIA IRANICA

Estimation of Mean Radius, Length and Density of Microvasculature Using Diffusion and Perfusion MRI

M. Ashoor*, M. Jahed[1], M. Chopp[2] and A. Mireshghi[3]

In theory, diffusion and perfusion information in MRI maps can be combined to yield morphological information, such as capillary density, volume and possibly capillary plasma velocity. This paper suggests a new method for determination of mean radius, length and capillary density in normal regions using diffusion and perfusion MRI. Mean Transit Time (MTT), Cerebral Blood Volume (CBV), Apparent Diffusion Coefficient (ADC), pseudo-diffusion coefficient (D^*) and ΔR_2 and ΔR_2^* values were utilized to calculate mean radius, length and capillary density. To verify the proposed theory, a special protocol was designed and tested on normal regions of a male Wistar rat using obtained functions. Mean radius, length and capillary density in the normal regions were calculated to be 2.48 ± 0.35 (mean $\pm$ SD), 234 ± 12 microns and $11897 \pm 219/\text{mm}^3$, respectively. With respect to the values 0.01 through 0.1 for the $\text{CBV}/\text{Vol}_{(\text{voxel})}$ parameter and 1 through 1000 sec for $\Delta R_2^{*2}/\Delta R_2^3$, the mean radius of the capillary, using the proposed method, varied from 0.076 to 7.58 microns.

INTRODUCTION

As an alternative to traditional techniques for measuring such parameters as capillary density and characterizing microvascular morphology, non-invasive Magnetic Resonance Imaging (MRI) techniques, with contrast weighting sensitive to micro-vasculature characteristics, have been proposed [1]. For instance, an approach suggested by Dennie et al., which measures changes in the spin-spin suggested relaxation rates $1/T_2(\Delta R_2)$ and $1/T_2^*(\Delta R_2^*)$, caused by the injection of a blood pool restricted contrast agent, has been proposed to be sensitive to microvessel density. An image is formed by mapping the ratio $\Delta R_2^*/\Delta R_2$, which is believed to be proportional to the product of the diffusion constant of water and microvascular density. However, the ratio $\Delta R_2^*/\Delta R_2$ depends, when contrast agent concentration is high, not just on microvascular properties, but also, on contrast agent concentration [2]. This may be a disadvantage, since concentration can be difficult to estimate accurately.

Another imaging technique [3], which is not contrast agent concentration-dependent, is proposed, in which the contrast is correlated to the morphology of capillaries and other small blood vessels. Again, the technique is based on measurements of the spin-spin relaxation rates, $1/T_2$ and $1/T_2^*$, before and after the injection of a contrast agent. An image is then formed by mapping the quantity: $Q = \Delta R_2/(\Delta R_2^*)^{2/3}$. This leads to a simple analytic formula for Q that involves only vessel density, water diffusion rate and distribution of the vessel radii: $Q \approx 1.678(DN)^{1/3}\langle R^{4/3}\rangle\langle R^2\rangle^{2/3}$, where R is the radius of the cylinder (capillary), N is the histological vessel (cylinder) density and D is the diffusion constant of water. Thus, "Q-maps" may yield information about capillary density, raising the possibility that Q may be a good indicator of angiogenesis. However, this expression does not yield a value for mean microvascular radius in the tissue.

Van Rijswijk et al. have reported that Apparent Diffusion Coefficient (ADC) values of all tumors, subcutaneous fat and muscle were significantly higher than

*. *Corresponding Author, Department of Mechanical Engineering, Sharif University of Technology, Tehran, I.R. Iran.*

1. *Department of Electrical Engineering, Sharif University of Technology, Tehran, I.R. Iran.*
2. *Department of Neurology, Henry Ford Health Sciences Center, Detroit, MI, USA; and Department of Physics, Oakland University, Rochester, MI, USA.*
3. *Department of Mechanical Engineering, Sharif University of Technology, Tehran, I.R. Iran.*

true diffusion coefficients, indicating a contribution of perfusion to the ADC. Also, true diffusion measurements, which are corrected for the perfusion effect, have the potential to be used as a noninvasive parameter in the characterization of soft-tissue masses [4], therefore, resulting in the assessment that a combination of diffusion and perfusion parameters may characterize the geometrical parameters of capillaries.

Capillaries, consisting of single layer endothelial cells, permit a rapid exchange of water and solutes with interstitial fluid, forming an interconnecting network of tubes of different lengths. Capillary distribution varies from tissue to tissue. In metabolically active tissues, capillaries are numerous, whereas, in less active tissues, capillary density is low. Therefore, geometry evaluation of capillaries can be useful and important.

At present, the relationship between capillary geometry and perfusion and diffusion information, such as Cerebral Blood Flow (CBF), Cerebral Blood Volume (CBV), ADC, Mean Transit Time (MTT) and ΔR_2^* and ΔR_2 values, is not fully established. The combination of CBV, ADC, MTT, ΔR_2^* and ΔR_2 values may allow a certain descriptive assessment related to microvascular geometry, such as mean radius, length and capillary density. In this study, through introduction of a preliminary function using the above parameters, along with a suitable set of hypotheses, a new descriptive qualifier, related to microvascular geometry, such as mean radius, length and capillary density, is introduced.

METHODS

Theory

A paramagnetic or super paramagnetic contrast agent introduced in the vascular compartment creates an additional susceptibility difference ($\Delta\chi$) between blood vessels and surrounding tissues and the blood fraction, ξ_0, may be determined from ΔR_2^* measurements, if the blood concentration of contrast agent (and, hence, $\Delta\chi$) is known,

$$\xi_0 = \frac{3}{4\pi}.\frac{\Delta R_2^*}{\gamma.\Delta\chi.B_0}, \tag{1}$$

where B_0 is the magnetic field strength of the external magnetic field and γ is the proton gyromagnetic ratio. A spin-echo experiment yields information on the vessel size distribution and the Vessel Size Index, (VSI), can be written as:

$$r = 0.425 \times \left(\frac{D}{\gamma.\Delta\chi.B_0}\right)^{1/2}.\left(\frac{\Delta R_2^*}{\Delta R_2}\right)^{3/2}. \tag{2}$$

Absolute measurement of radius (r) requires measurement (or prior knowledge) of the diffusion coefficient and of the increase in blood susceptibility, due to the contrast agent injection [5]. The index of the Total Capillary Length (TCL) is defined as follows:

$$\text{TCL} = \frac{\xi_0}{\pi r^2}.\text{Vol(voxel)}. \tag{3}$$

By combining Equations 1 to 3, one obtains:

$$\text{TCL} = 420.7\frac{1}{D}.\frac{\Delta R_2^3}{\Delta R_2^{*2}}.\text{Vol(voxel)}. \tag{4}$$

If the capillaries are assumed to be cylinders with mean length (ℓ) and mean radius (r), then, CBV may be approximated as:

$$N \cong \text{CBV} \times (\pi.\ell.r^2)^{\ 1}, \tag{5}$$

where N is the number of capillaries [6]. Arranging the cylindrical capillary segments in a series format, namely $N.\ell$, provides the notion that this value is practically equal to TCL. Hence, by combining Equations 4 and 5, one obtains:

$$r_{(\mu m)} = \left(7.57 \times 10^3 \frac{D.\text{CBV}}{\text{Vol(voxel)}}.\frac{\Delta R_2^{*2}}{\Delta R_2^3}\right)^{1/2}. \tag{6}$$

An experimental assessment of CBV, CBF and MTT can be outlined as follows: CBV can be defined as a volume fraction: CBV (%) = 100 × (volume of blood in a voxel)/(volume of the voxel). CBF is defined as the net blood flow through the voxel divided by the mass of the voxel. The used unit for CBF is milliliters per 100 grams of tissue per minute. The MTT describes the average amount of time it takes any water molecule or particle of contrast agent to pass through the voxel vasculature. MTT is generally expressed in seconds and is given by MTT = CBV/CBF [7].

If the TCL is the Total Capillary Length, one has, according to the definition of the MTT in the capillary network, the following:

$$\begin{aligned}\text{MTT} &= \text{TCL} \times V^{\ 1} = (\text{TCL}).\ell \times (6.D^*)^{\ 1} \\ &= \text{CBV} \times \text{CBF}^{\ 1},\end{aligned} \tag{7}$$

where, as before, ℓ is the mean capillary segment length, defined as the average distance along which spins move with a constant velocity (V) and D^* is pseudo-diffusion coefficient [8]. The quantity ($< \ell >< V > /6$) has the dimension of a diffusion coefficient and has been referred to as pseudo-diffusion coefficient D^*. By combining Equations 4 to 7, one obtains,

$$V_{(m/s)} = 420.7\frac{1}{D.\text{MTT}}.\frac{\Delta R_2^3}{\Delta R_2^{*2}}.\text{Vol(voxel)}, \tag{8}$$

$$\ell_{(mm)} = 142.62\frac{D.D^*.\text{MTT}}{\text{Vol(voxel)}}.\frac{\Delta R_2^{*2}}{\Delta R_2^3}, \tag{9}$$

$$N_{(1/mm^3)} = 0.295 \frac{\text{Vol(voxel)}}{D^2.D^*.\text{MTT}} \cdot \left(\frac{\Delta R_2^{*2}}{\Delta R_2^3}\right)^2. \quad (10)$$

Using literature data for $< \ell >$ and $< V >$ [7], D^* is expected to be about eight to ten times larger than the true diffusion coefficient of water at room temperature ($D^* \cong 10D$) [9]. However, a currently precise measurement of D^* is not possible, in view of Signal to Noise Ratio (SNR) limitations. As such, this issue certainly requires further study, especially in the theoretical analysis domain. It is believed that $D^* \cong 10D$ is a good estimation and starting point for further analytical studies and, therefore, it has been utilized in the current study. Hence, now, based on the above estimation, Equations 9 and 10 can be rewritten as:

$$\ell_{(mm)} = 1426.2 \frac{D^2.\text{MTT}}{\text{Vol(voxel)}} \cdot \frac{\Delta R_2^{*2}}{\Delta R_2^3}, \quad (11)$$

$$N_{(1/mm^3)} = 2.95 \times 10^{\ 2} \frac{\text{Vol(voxel)}}{D^3.\text{MTT}} \cdot \left(\frac{\Delta R_2^{*2}}{\Delta R_2^3}\right)^2. \quad (12)$$

Finally, one can estimate mean radius, length and capillary density in normal regions using Equations 6, 11 and 12, respectively.

MRI Measurement Procedure

To evaluate the proposed theory and develop a test protocol, the following measurement was conducted on the normal vasculature regions of a male Wistar rat, using a 7 Tesla MRI system. Briefly, an aged white clot (prepared 24 h before ischemia) was slowly injected into the internal carotid artery to block the middle cerebral artery (MCA) [10]. MRI measurements were performed using a 7 T, 20 cm bore super conducting magnet (Magnex Scientific, Abingdon, UK) interfaced to a SMIS console (Surrey, England). A 12 cm bore actively shielded gradient coil set, capable of producing magnetic field gradients up to 20 gauss/cm, was used. The Radio Frequency (rf) pulses were applied by a 7.5 cm diameter saddle coil, actively decoupled by TTL control from the 1.4 cm surface receiver coil, which was positioned over the center line of the animal skull. Stereotaxic ear bars were used to minimize movement during the imaging procedure. During MRI measurements, anesthesia was maintained using a gas mixture of N_2O (69%), O_2 (30%) and halothane (1%). Rectal temperature was kept at 37 $\pm$ 0.5°C, using a feedback controlled water bath. A modified Fast Low Angle SHot (FLASH) [11] imaging sequence was employed for reproducible positioning of the animal in the magnet at each MRI session [12]. Diffusion Weighted Imaging (DWI) and Perfusion Weighted Imaging (PWI) measurements were performed 24 hrs after the onset of embolization.

T_2 was measured using a standard two-Dimensional Fourier Transform (2DFT) multi slice (seven slices) multi echo (four echo) MRI. A series of four sets of images (7 slices for each set) were obtained using TEs of 20, 40, 60 and 80 msec and a TR of 3 seconds. Images were produced using a 32 mm Field Of View (FOV), 2 mm slice thickness and 128×64 image matrix. The total time for the entire sequence was approximately 3.2 min. Transverse relaxation rates, R_2^*, R_2' and $R_2(1/T_2^*, 1/T_2'$ and $1/T_2)$, were measured using the Look-Locker sequence [13], which provides the data required to construct multi section maps of R_2^*, R_2' and R_2 in a single acquisition. For this study, five gradient echoes, with a first echo time of 10 msec and an interecho spacing of 8 msec, were acquired prior to the 180° pulse. The echo train, after the 180° pulse, contained six echoes separated by 8.1 msec. A series of eleven sets of images (7 slices for each set) were obtained using TEs of 98 msec and a TR of 3 seconds. Images were produced using a 32 mm FOV, 2 mm slice thickness and 128×128 image matrix. The total time for the entire sequence was approximately 6.4 min.

ADCw was measured using the Stejskal-Tanner sequence with three b-values (10, 800 and 1800 s/mm^2) in each of three diffusion sensitizing directions, seven slices, 32 mm FOV, 128×64 matrix, TR = 1.5 s and TE = 40 ms. Each image required a scan time of 3.2 min for completion. The total time for the entire sequence was, approximately, 14.4 min.

Perfusion measurements were performed prior to each diffusion measurement, using the arterial spin tagging technique [14]. Two images were obtained for perfusion measurement with parameters: TR = 1 sec, TE = 30 msec, 64×64 image matrix, 3 mm slice thickness and a 32 mm field of view. The animal PWI was measured within a coronal section, with coordinates centered at interaural 8.2 mm and bregma 0.8 mm [15]. The duration of the inversion pulse was 1 sec at a B1 amplitude of 0.3 KHz.

Data Analysis

The ROIs were selected for measurement of MRI parameters. The mean and Standard Deviations (SD) of ADCw values of the parenchymal tissue (not including Cerebrospinal Fluid (CSF)) in the contra lateral hemisphere were measured and the threshold values, to determine the number of pixels with abnormal values in the ipsilateral hemisphere, were defined using mean ADCw $1.5 \times$ SD in the contra lateral hemisphere, where this value is a heuristic one. With respect to the obtained ROIs, the mean and Standard Deviations (SD) of MTT, CBV, ΔR_2^* and ΔR_2 values of the parenchymal tissue in the contra lateral hemisphere

were also measured. A paired t-test was used to compare the two ROI's, with a significance level of 0.05.

RESULTS

With respect to the values 0.01 through 0.1 for the $\text{CBV/Vol}_{(\text{voxel})}$ parameter and 1 through 1000 sec for $\Delta R_2^{*2}/\Delta R_2^3$, the mean radius of the capillary using Equation 6 in the theory section, has been varied from 0.076 to 7.58 microns. Figure 1 depicts the relationship among the mean capillary radius, $\text{CBV/Vol}_{(\text{Voxel})}$ and CSSRT parameters, where CSSRT is the $\Delta R_2^{*2}/\Delta R_2^3$ value with the two different diffusion constants of water as 0.0007 mm^2/sec and 0.0004 mm^2/sec in the ROI of the rat's brain. As shown, by increasing the diffusion constant of the water, the mean capillary radius is increased. Figure 2 also depicts the relationship between the total capillary length, ADC, and ICSSRT parameters, where ICSSRT is the $\Delta R_2^3/\Delta R_2^{*2}$ value with three different voxel volume values; 1, 8 and 27 mm^3. As shown with increasing voxel volume, total capillary length is increased.

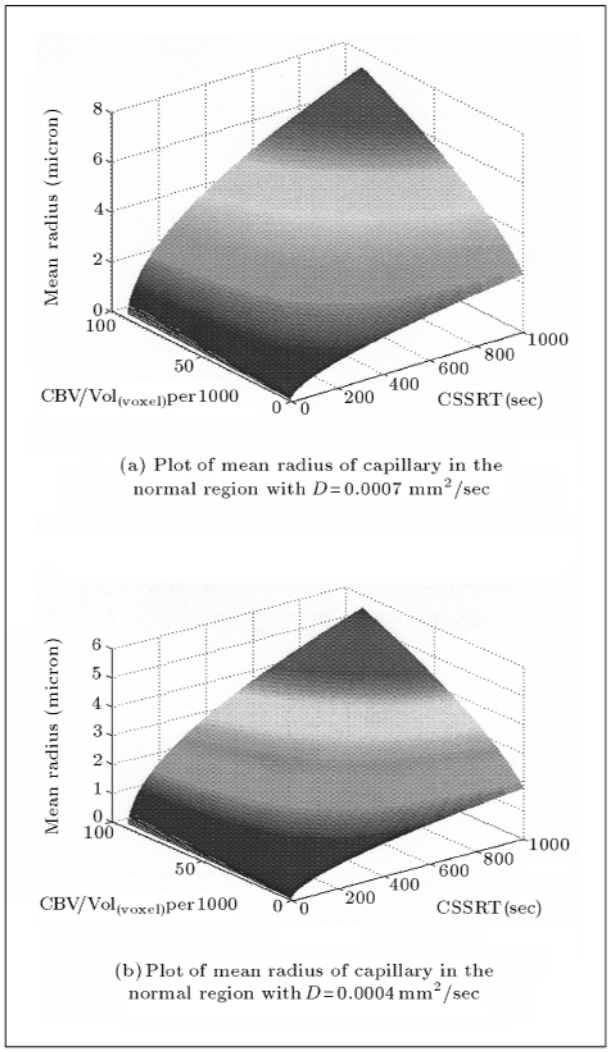

Figure 1. Plots showing the relationship between mean capillary radius, $\text{CBV/Vol}_{(\text{Voxel})}$ and CSSRT parameters where CSSRT is $\Delta R_2^{*2}/\Delta R_2^3$ value with the diffusion constant of water. As shown, by increasing diffusion constant of water, mean capillary radius is increased.

For the calculation of ADC, the mono-exponential intra-voxel incoherent motion model was used, $S(b) = S(0) \times \exp(\ b \times \text{ADC})$ [12]. Because the diffusion of water may be directionally dependent (anisotropic), measurement in only one direction can lead to incorrect image interpretation. The diffusion gradient was, therefore, applied in each of three orthogonal directions (x, y, z), and an average of these measurements was calculated to give the trace of the diffusion tensor, which is reported to minimize the effects of diffusion anisotropy [16]. Figure 3 depicts known maps (ADC, CBV, MTT, ΔR_2^* and ΔR_2) utilizing noise reduction and artifact cancellation algorithms.

Using the ROIs in the normal regions on the upper maps, the perfusion and diffusion parameters have been measured as MTT = 3.19 $\pm$ 0.28 sec, $\text{CBV/Vol}_{(\text{voxel})}$ = 0.058 $\pm$ 0.012, ΔR_2 = 3.56 $\pm$ 0.3 sec^{-1}, ADC = 0.00064 $\pm$ 0.00007 $\text{mm}^2\text{sec}^{-1}$, $\text{Vol}_{(\text{voxel})}$ = 0.3125 $\times$ 0.3125 $\times$ 2 mm^3 and ΔR_2^* = 33.7 $\pm$ 3 sec^{-1}, using the obtained maps. Mean radius, length and capillary density in normal regions, using Equations 6, 11 and 12, were calculated to be 2.48 $\pm$ 0.35 (mean $\pm$ SD), 234 $\pm$ 12 microns and 11897 $\pm$ 219/mm^3, respectively. For normal regions, the results are shown in Table 1, depicting the radius, length and density of the microvasculature in capillary space.

DISCUSSION

It has been shown that mean radius, length and capillary density are dependent on the ADC, CBV, MTT, D^* and $\Delta R_2^{*2}/\Delta R_2^3$ parameters. This study provides key specifications of the microvasculature through appropriate hypotheses, using diffusion and perfusion MRI. These results have been verified through mi-

Table 1. Geometrical specifications of capillaries in the normal region of rat's brain.

Mean Capillary Length ℓ	0.234 $\pm$ 0.012 mm
Capillary Density (N)	11897 $\pm$ 219/mm^3
Mean Capillary Radius (r)	2.48 $\pm$ 0.35 μm

Results are presented for normal regions where mean length, radius and density of capillary have been calculated using measured parameters such as MTT = 3.19 $\pm$ 0.28 sec, $\text{CBV/Vol}_{(\text{voxel})}$ = 0.058 $\pm$ 0.012, ΔR_2 = 3.56 $\pm$ 0.3 sec^{-1}, ADC = 0.00064 $\pm$ 0.00007 $\text{mm}^2\text{sec}^{-1}$, $\text{Vol}_{(\text{voxel})}$ = 0.3125 $\times$ 0.3125 $\times$ 2 mm^3 and ΔR_2^* = 33.7 $\pm$ 3 sec^{-1}.

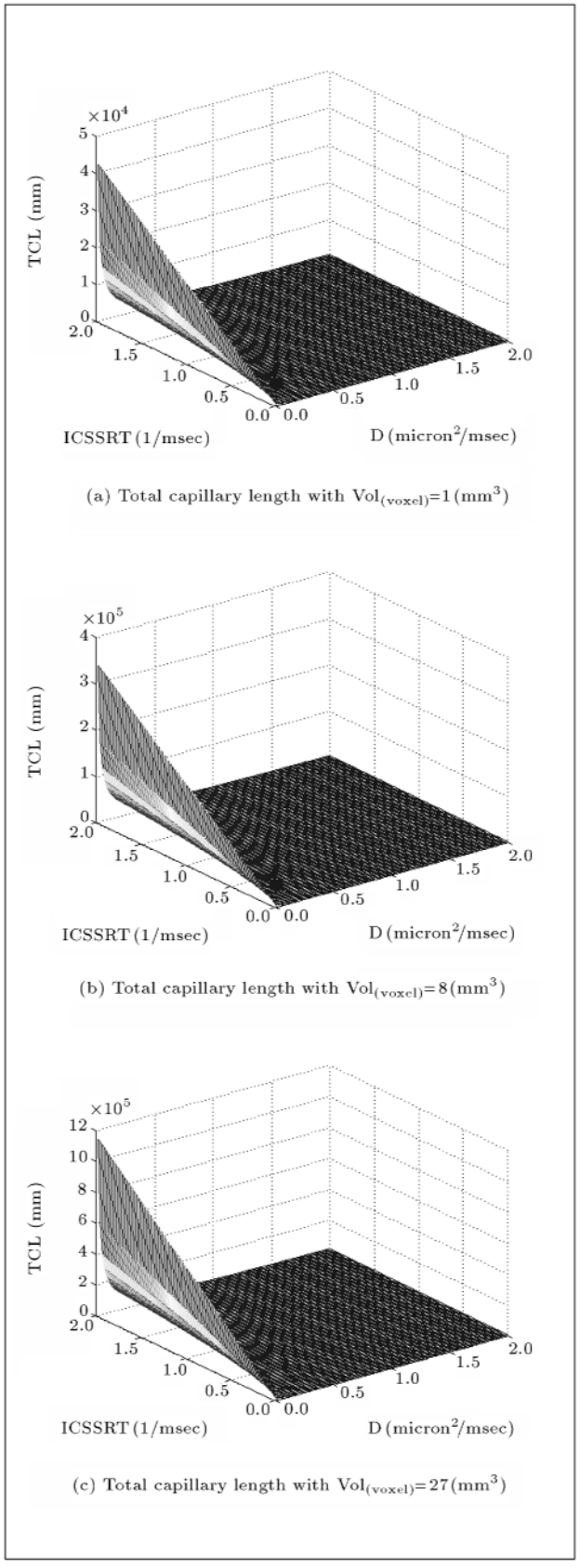

Figure 2. Plots showing the relationship between TCL, D and $\Delta R_2^3/\Delta R_2^{*2}$ with volume voxel. As shown, by increasing volume voxel TCL is increased.

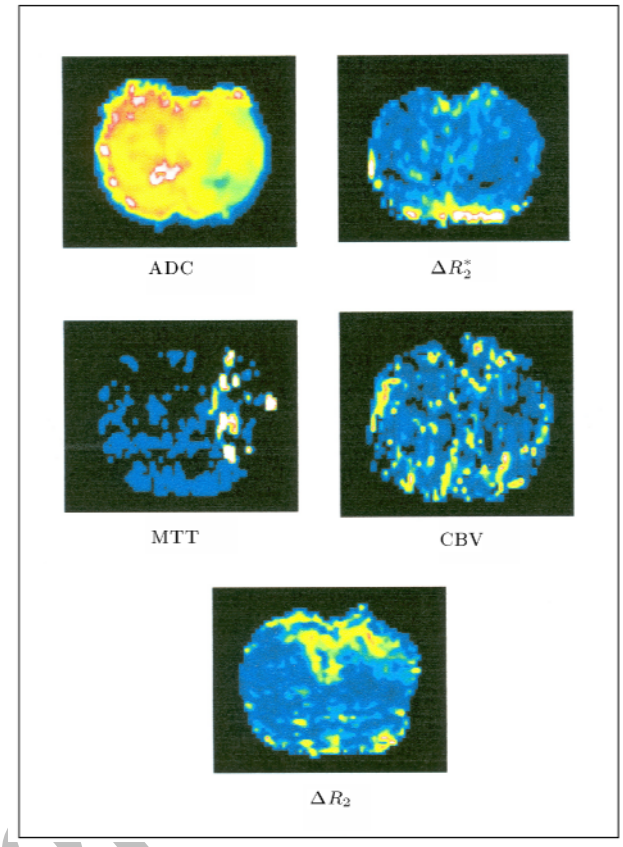

Figure 3. ADC, MTT, ΔR_2 , ΔR_2^* and CBV maps. Left side of all images is normal and selected ROIs are based on the right side that is a damaged region.

croscopy methods and in various published material on this subject [17-21]. Pathak et al. showed that, in the normal contra-lateral section of the brain, the mean vessel length and mean vessel radius were 178.59 $\pm$ 28.76 and 3.72 $\pm$ 0.72 microns, respectively [18].

The ADC is a weighted average of the diffusion coefficients of the intracellular and interstitial compartments. The diffusion coefficients for two separate compartments, Dint (interstitial) and Din (intracellular), are given in the literature as Dint = 0.00325 mm^2s^{-1} and Din = 0.000143 mm^2s^{-1}. In a normal brain, the interstitial space volume is 20% of the total volume, whereas the intracellular compartment comprises approximately 80% of the total volume. Thus, for a normal brain, one would calculate an average weighted diffusion coefficient of $0.2 \times 0.00325 + 0.8 \times 0.000143$ mm^2s^{-1}, or 0.00076 mm^2s^{-1} [22,23]. The authors measured value is in agreement with this result. Mean radius, length and capillary density are depended on this parameter.

Energy depletion, temperature, intracellular water accumulation, changes in tortuosity of the extra cellular diffusion paths and changes in cell membrane permeability have all been implicated as contributing to the changes in ADCw. The increase in ADCw

appears to occur concomitantly with loss of membrane structure and loss of barriers to diffusion [24]. The decreased ADCw is associated with a specific threshold level of regional cerebral blood flow, similar to that which is associated with the loss of membrane potential and is, also, associated with breakdown of energy metabolism, acidosis, cellular ionic shifts and decreased Na+, K+-ATPase activity [25]. ADC values of normal cortex and caudate-putamen were $(726 \pm 22) \times 10^{-6}$ mm^{2}s^{-1} and $(659 \pm 17) \times 10^{-6}$ mm^{2}s^{-1}, respectively [26]. This, however, is again, in agreement with the results obtained in this study. As shown in Figure 1, with increasing ADC, mean capillary radius will be increased.

Background imaging gradients, gradient linearity, refocusing RF pulses, eddy currents, image misregistration, noise and dynamic range contribution, as systemic sources of error, may affect estimation of the ADC value. Also, microscopic, biophysical tissue properties, partial volume effects, anisotropy, restriction, diffusion distance, compartmentation, exchange, multiexponential diffusion decay, T_2 weighting and microvascular perfusion are responsible for ADC inaccuracy [27]. In general, they affect estimation of the static and dynamic specifications of the capillary, which is not in the scope of this study.

Quantity $\Delta R_2^{*2}/\Delta R_2^3$ plays a major role in the quantification of the dynamic and static specifications of capillaries in perfusion and diffusion MRI. Generally, in such quantification, slow rhythm and static dephasing are included. As this quantity is increased, for a constant CBV/Vol$_{(\text{voxel})}$ in capillary space, mean capillary radius is also increased. Such an increase will accelerate as CBV/Vol$_{(\text{voxel})}$ is further increased. In general, maximum (minimum) mean capillary radius occurs when $\Delta R_2^{*2}/\Delta R_2^3$ and CBV/Vol$_{(\text{voxel})}$ are both maximized (minimized). On the other hand, (maximum) mean capillary radius is directly related to ADC. In regard to the capillary length, as such quantity is variable, it is directly related to effective voxel volume, $\Delta R_2^3/\Delta R_2^{*2}$ and ADC.

ACKNOWLEDGMENTS

The authors wish to extend their gratitude and thanks to Drs. Zheng Gang Zhang, Quan Jiang and James R. Ewing for technical assistance and to the Department of Neurology's NMR Facility at Henry Ford Health Sciences Center in Detroit, Michigan, for providing the means and support required for the implementation of this study.

REFERENCES

1. Van Dijke, C.F., Brasch, R.C., Roberts, TPL., Weidner, N., Mathur, A., Shames, D.M., Mann, J.S., Demsar, F., Lang, P. and Schwickert, H.C. "Mammary carcinoma model: Correlation of macromolecular contrast-enhanced MR imaging characterizations of tumor microvasculature and histologic capillary density", *Radiology*, **198**, pp 813-818 (1996).
2. Dennie, J., Mandeville, J.B., Boxerman, J.L., Packard, S.D., Rosen, B.R. and Weisskoff, R.M. "NMR imaging of changes in vascular morphology due to tumor angiogenesis", *Magnetic Resonance in Medicine*, **40**, pp 793-799 (1998).
3. Jensen, J.H. and Chandra, R. "MR imaging of microvasculature", *Magn. Reson. Med.*, **44**, pp 224-230 (2000).
4. Van Rijswijk, C.S.P., Kunz, P., Hogendoorn, P.C.W., Taminiau, A.H.M., Doornbos, J. and Bloem, J.L. "Diffusion-weighted MRI in the characterization of soft-tissue tumors", *Journal of Magnetic Resonance Imaging*, **15**, pp 302-307 (2002).
5. Tropres, I., Grimault, S., Vaeth, A., Grillon, E., Julien, C., Payen, J.F., Lamalle, L. and Decorps, M. "Vessel size imaging", *Magn. Reson. Med.*, **45**, pp 397-408 (2001).
6. Ashoor, M., Jiang, Q., Chopp, M. and Jahed, M. "Introducing a new definition towards clinical detection of microvascular changes using diffusion and perfusion MRI", *Scientia Iranica*, Sharif University of Technology, **12**(1), pp 109-115 (2005).
7. Barbier, E.L., Lamalle, L. and Decorps, M. "Methodology of brain perfusion imaging", *Journal of Magnetic Resonance Imaging*, **13**, pp 496-520 (2001).
8. Bihan, D.L., *Diffusion and Perfusion Magnetic Resonance Imaging*, Raven Press, Ltd. New York, chapter 15, pp 270-274 (1995).
9. Bihan, D.L. "Molecular diffusion nuclear magnetic resonance imaging", *Magn. Reson. Med.*, **7**(1), pp 1-30 (1991).
10. Zhang, R., Chopp, M., Zhang, Z., Jiang, Q. and Ewing, J.R. "A rat model of embolic focal cerebral ischemia", *Brain Research*, **766**, pp 83-92 (1997).
11. Haase, A., Frahm, J., Matthaei, D., Hanicke, W. and Merboldt, K.D. "FLASH imaging. Rapid NMR imaging using low flip-angle pulses", *J. Mag. Res.*, **67**, pp 258-266 (1986).
12. Jiang, Q., Zhang, Z.G., Chopp, M., Helpern, J.A., Ordidge, R.J., Garcia, J.H., Marchese., B.A., Qing, Z.X. and Knight, R.A. "Temporal evolution and spatial distribution of the diffusion constant of water in rat brain after transient middle cerebral artery occlusion", *Journal of the Neurol Sci.*, **120**, pp 123-130 (1993).
13. Ma, J. and Wehrli, F.W. "Method for image-based measurement of the reversible and irreversible contribution to the transverse-relaxation rate", *J. Magn. Reson.*, **B 111**, pp 61-69 (1996).
14. Williams, D., Detre, J., Leigh, J. and Koretsky, A. "Magnetic resonance imaging of perfusion using spin inversion of arterial water", *Proc. Nat'l. Acad. Sci.*, USA, **89**, pp 212-216 (1992).

15. Paxinos, G. and Watson, C., *The Rat Brain in Stereotaxic Coordinates*, 2nd Eds., Academic Press (1986).

16. Barber, P.A., Darby, D.G., Desmond, P.M., Yang, Q., Gerraty, R.P., Jolley, D., Donnan, G.A., Tress, B.M. and Davis, S.M. "Prediction of stroke outcome with echo planar perfusion- and diffusion-weighted MRI", *Neurology*, **51**, pp 418-426 (1998).

17. Bihan, D.L. and Turner, R. "The capillary network: A link between IVIM and classical perfusion", *Magn. Reson. Med.*, **27**, pp 171-178 (1992).

18. Pathak, A.P., Schmainda, K.M., Ward, B.D., Linderman, J.R., Rebro, K.J. and Greene, A.S. "MR-derived cerebral blood volume maps: Issues regarding histological validation and assessment of tumor angiogenesis", *Magn. Reson. Med.*, **46**, pp 735-747 (2001).

19. Gesztelyi, G., Finnegan, W., De Maro, J.A., Wang, J., Chen, J. and Fenstermacher, J. "Parenchymal microvascular systems and cerebral atrophy in spontaneously hypertensive rats", *Brain Research*, **611**, pp 249-257 (1993).

20. Lin, S.Z., Sposito, N., Pettersen, S., Rybacki, L., McKenna, E., Pettigrew, K. and Fenstermacher, J. "Cerebral capillary bed structure of normotensive and chronically hypertensive rats", *Microvascular Research*, **40**, pp 341-357 (1990).

21. Dunn, J.F., Roche, M.A., Springett, R., Abajian, M., Merlis, J., Daghlian, C.P., Lu, S.Y. and Makki, M. "Monitoring angiogenesis in brain using steady-state quantification of ΔR_2 with MION infusion", *Magn. Reson. Med.*, **51**, pp 55-61 (2004).

22. Benveniste, H., Hedlund, L.W. and Johnson, A. "Mechanism of detection of acute cerebral ischemia in rats by diffusion-weighted magnetic resonance microscopy", *Stroke*, **23**, pp 746-754 (1992).

23. Bihan, D.L., Moonen, C.T.W., Van Zijl, P.C.M., Pekar, J. and Des Pres, D. "Measuring random microscopic motion of water in tissues with MR Imaging: A cat brain study", *Journal of Computer Assisted Tomography*, **15**, pp 19-25 (1991).

24. Jiang, Q., Chopp, M., Zhang, Z.G., Knight, R.A., Jacobs, M., Windham, J.P., Peck, D., Ewing, J.R. and Welch, K.M.A. "The temporal evolution of MRI tissue signatures after transient middle cerebral artery occlusion in rat", *Journal of the Neurological Sciences*, **145**, pp 15-23 (1997).

25. Welch, K.M.A., Windham, J., Knight, R.A., Nagesh, V., Hugg, J.W., Jacobs, M., Peck, D., Booker, P., Dereski, M.O. and Levine, S.R. "A model to predict the histopathology of human stroke using diffusion and T2-weighted magnetic resonance imaging", *Stroke*, **26**, pp 1983-1989 (1995).

26. Hoehn-Berlage, M., Norris, D.G., Kohno, K., Mies, G., Leibfritz, D. and Hossmann, K.A. "Evolution of regional changes in apparent diffusion coefficient during focal ischemia of rat brain: The relationship of quantitative diffusion NMR imaging to reduction in cerebral blood flow and metabolic disturbances", *Journal of Cerebral Blood Flow and Metabolism*, **15**, pp 1002-1011 (1995).

27. Conturo, T.E., McKinstry, R.C., Aronovitz, J.A. and Neil, J.J. "Diffusion MRI: Precision, accuracy and flow effects", *NMR in Biomedicine*, **8**, pp 307-332 (1995).